

# Synthesis of SAPO-34 with only Si(4Al) species: Effect of Si contents on Si incorporation mechanism and Si coordination environment of SAPO-34

Lei Xu<sup>a,b</sup>, Aiping Du<sup>a</sup>, Yingxu Wei<sup>a</sup>, Yingli Wang<sup>a,b</sup>, Zhengxi Yu<sup>a,b</sup>, Yanli He<sup>a</sup>,  
Xinzhi Zhang<sup>a</sup>, Zhongmin Liu<sup>a,\*</sup>

<sup>a</sup> Dalian Institute of Chemical Physics, Chinese Academy of Sciences, Dalian 116023, China

<sup>b</sup> Graduate University of Chinese Academy of Sciences, Beijing 100049, China

Received 12 December 2007; received in revised form 30 January 2008; accepted 2 February 2008

Available online 10 February 2008

## Abstract

SAPO-34 molecular sieves with different Si coordination environment were synthesized by adjusting SiO<sub>2</sub>/Al<sub>2</sub>O<sub>3</sub> molar ratio in starting gel. The crystal structure, element composition and Si coordination environment of the as-synthesized samples were characterized by XRD, SEM, XRF and NMR. SAPO-34 molecular sieve could be obtained when the SiO<sub>2</sub>/Al<sub>2</sub>O<sub>3</sub> molar ratio of the starting gel was higher than 0.075. The content and modeling of Si incorporated into SAPO-34 framework varied with the SiO<sub>2</sub>/Al<sub>2</sub>O<sub>3</sub> molar ratios in the starting gel and different Si chemical environments were formed correspondingly. SAPO-34 with only Si(4Al) coordination structure could be prepared when the SiO<sub>2</sub>/Al<sub>2</sub>O<sub>3</sub> molar ratio of the starting gel was in range of 0.075–0.15.  
© 2008 Elsevier Inc. All rights reserved.

**Keywords:** SAPO-34; Si incorporation mechanism; Si coordination environment

## 1. Introduction

SAPO-34 molecular sieves, with 8-ring pore opening and medium-strong acidity, showed excellent performance in catalytic conversion of methanol to light olefins (MTO) [1–3]. This provided a potential way for developing a commercial MTO process to produce light olefins from coal or natural gas, as an alternative to the conventional oil route. In the past two decades, MTO reaction over SAPO-34 catalyst has been an important topic in academic and industrial fields. The structure, acidity and catalytic performance of SAPO-34 directly depend on the number and distribution of Si in the framework [4–6], which is related closely to Si incorporation mechanism and coordination environment.

The acidity of SAPO molecular sieve is generated by the surface bridge hydroxyl group, which originates from the protons for compensating the unbalanced electric charges due to Si incorporation into the neutral framework of AlPOs molecular sieve. Many researchers have studied the mechanism of Si incorporation into AlPOs framework and the Si substitution mechanism is generally recognized in the crystallization process of SAPO molecular sieve [5,7–9]. First, AlPOs structure was formed, then Si atoms was incorporated into the AlPOs framework by isomorphous substitution. It is a general rule that the linkage of the type Si–O–P is avoided. Thus, Si was incorporated into AlPOs framework by two different substitution mechanisms: (1) SM2 substitution mechanism, the replacement of phosphorus by silicon; (2) SM3 substitution mechanism, the double substitution of neighboring aluminum and phosphorus by two Si atoms [4]. Prakash proposed that Si incorporation by the first mechanism formed Si(4Al) structures when the SiO<sub>2</sub>/Al<sub>2</sub>O<sub>3</sub> molar ratio was low in

\* Corresponding author. Tel.: +86 411 84685510; fax: +86 411 84379289.

E-mail address: [liuzm@dicp.ac.cn](mailto:liuzm@dicp.ac.cn) (Z. Liu).

starting gel, while for a starting gel with increasing  $\text{SiO}_2/\text{Al}_2\text{O}_3$  molar ratio, Si(3Al), Si(2Al), Si(1Al) and Si(0Al) structures were formed simultaneously by the second mechanism [9]. It is recognized that the Si coordination structures has significant effect on the acid intensity of SAPO molecular sieve, which was enhanced in the order of  $\text{Si}(0\text{Al}) < \text{Si}(4\text{Al}) < \text{Si}(3\text{Al}) < \text{Si}(2\text{Al}) < \text{Si}(1\text{Al})$  [10]. In our previous work [11], The results showed that Si atoms were incorporated into the framework of as-synthesized SAPO-34 with higher Si content ( $\text{SiO}_2/\text{Al}_2\text{O}_3 = 0.6$ ) by two mechanisms in different crystallization stages. In the earlier stage of the crystallization, Si, P and Al formed crystal nucleuses by the crystallization mechanism of direct participation, and only Si(4Al) species are found in the framework structure. In the growth period of the crystal grains, the remaining small amount of Si in the gel is incorporated into the framework to form Si-rich species by SM2 and SM3 substitution mechanisms and the amount of Si(4Al) increases slightly and Si(3Al), Si(2Al), Si(1Al) and Si(0Al) are formed. This indicated that during the SAPO-34 crystallization, SM2 and SM3 substitutions take place simultaneously until Si contents of SAPO-34 framework were up to a threshold value.

These observations interested us to investigate the mechanism of Si incorporation into SAPO-34 as-synthesized with various Si content in the starting gel with a long crystallization period. These investigations provide the possibility to adjust Si coordination structure by controlling Si content in the starting gel. In the present work, SAPO-34 molecular sieves with different Si coordination environments were synthesized by adjusting  $\text{SiO}_2/\text{Al}_2\text{O}_3$  molar ratios of the starting gels. The mechanism of Si incorporation for forming different Si coordination environments was discussed.

## 2. Experimental

SAPO-34 was synthesized by a hydrothermal method from a gel molar composition of  $3.0\text{R}:1.0\text{Al}_2\text{O}_3:x\text{SiO}_2:1.0\text{-P}_2\text{O}_5:50\text{H}_2\text{O}$ , where R is a templating agent and  $x$  is equal to 0.025, 0.075, 0.10, 0.15, 0.20 and 0.60. Pseudoboehmite (72 wt%  $\text{Al}_2\text{O}_3$ ), orthophosphoric acid (85 wt%  $\text{H}_3\text{PO}_4$ ) and silica sol (25 wt%  $\text{SiO}_2$ ) were used as the starting materials to get aluminum, phosphorus and silicon, respectively. The templating agent was triethylamine (TEA). Pseudoboehmite was dissolved in deionized water to form alumina sol, and then silica sol was added to the prepared alumina sol under stirring. Orthophosphoric acid was then added slowly under continual stirring for 10 min. After that, triethylamine was added to the prepared mixture, and stirred for 20 min until attaining a homogeneous gel mixture. The gel mixture was sealed in 200 ml Teflon-lined stainless steel pressure vessels and heated in an oven at  $200^\circ\text{C}$  under autogenic pressure for 24 h. After crystallization, as-synthesized samples were obtained after centrifugal separation, washing, and drying at  $120^\circ\text{C}$ , which were

denoted as SP-0.025, SP-0.075, SP-0.10, SP-0.15, SP-0.20 and SP-0.60, respectively.

X-ray power diffraction (XRD) patterns were recorded on a RIGAKU D/max-rb Diffractometer using  $\text{Cu K}\alpha$  radiation with nickel filter. SEM photographs were obtained on a KYKY-AMRAY-1000B scanning electron microscopy. X-ray fluorescence analysis (XRF) was performed on a Philips Magix-601 X-Ray Fluorescence Spectrometer. All NMR spectra were recorded at room temperature on a Bruker DRX-400 spectrometer with BBO MAS probehead using 4 mm  $\text{ZrO}_2$  rotors. The  $^{31}\text{P}$  MAS NMR spectra with high-power proton decoupling were performed at 161.9 MHz, using a 2.0  $\mu\text{s}$  pulse, a 2 s repetition time, and 4096 scans. Spinning speed was 8 kHz and chemical shift was referenced to 85% phosphoric acid which has a chemical shift of 0 ppm from TMS. The  $^{29}\text{Si}$  MAS NMR spectra with high power proton decoupling were obtained at 79.49 MHz using a 0.8  $\mu\text{s}$  pulse, a 4 s repetition time, and 2000 scans. Spinning speed was 4 kHz and chemical shift was referenced to 4,4-dimethyl-4-silapentane sulfonate sodium (DDS) which has a chemical shift of 0 ppm from TMS.

## 3. Results and discussion

### 3.1. Crystalline structure analysis

Fig. 1 presents XRD patterns of as-synthesized samples of SP-0.025, SP-0.075, SP-0.10, SP-0.15, SP-0.20 and SP-0.60, in which the sample codes correspond to the  $\text{SiO}_2/\text{Al}_2\text{O}_3$  molar ratios in the starting gel. It was found that SAPO-18 molecular sieve with AEI topological structure was formed when the  $\text{SiO}_2/\text{Al}_2\text{O}_3$  molar ratio of the starting gel was the lowest (0.025) [12–16]. SAPO-34 molecular

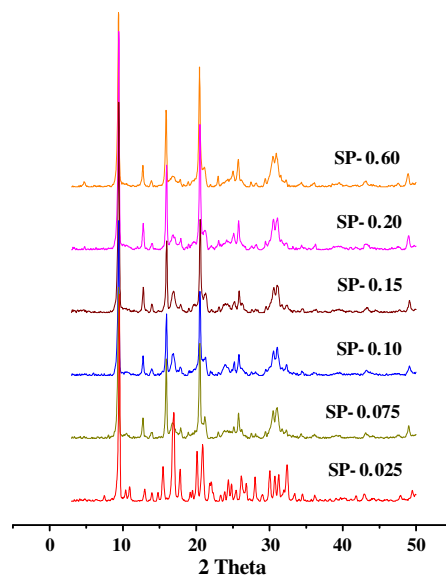


Fig. 1. XRD patterns of the as-synthesized products from the starting gel with different  $\text{SiO}_2/\text{Al}_2\text{O}_3$  ratios.

sieves with CHA topological structure could be obtained when the  $\text{SiO}_2/\text{Al}_2\text{O}_3$  molar ratio was higher than 0.075. The topological structure figures of AEI and CHA are depicted in Fig. 2 [17]. Both structures have the same periodic building units of double six ring (D6 R) layers (Fig. 2a), which are interconnected forming different 8-ring opening. The AEI and CHA topological structure are formed because of the different connection mode through the oxygen bridges, dissymmetry mode for CHA (Fig. 2b) or mirror symmetry for AEI (Fig. 2c). Although the same primary building units existed in the framework of SAPO-34 and SAPO-18 molecular sieves, the connection mode through the oxygen bridges can be changed by adjusting the  $\text{SiO}_2/\text{Al}_2\text{O}_3$  molar ratios of the starting gel. Apparently, the AEI topological structure was formed easily when the  $\text{SiO}_2/\text{Al}_2\text{O}_3$  molar ratio is low. With the increase of the  $\text{SiO}_2/\text{Al}_2\text{O}_3$  molar ratio, SAPO-34 with the CHA topological structure is obtained.

Fig. 3 presents the  $^{31}\text{P}$  MAS NMR spectra of the as-synthesized samples with different  $\text{SiO}_2/\text{Al}_2\text{O}_3$  molar ratios in the starting gel. In  $^{31}\text{P}$  MAS NMR spectra, SAPO-18

molecular sieves exhibited two resonance peaks at  $-29$  and  $-12$  ppm. The former one comes from the overlapping peaks of  $\text{P}_1$  and  $\text{P}_2$  species with the  $\text{P}(4\text{Al})$  structures. The latter one comes from  $\text{P}_3$  species [16,18]. As for SAPO-34 molecular sieves, only one resonance peak was shown at  $-29$  ppm. It could be concluded that only one kind of P chemical environment existed in SAPO-34 molecular sieves. However, a weakened resonance peak at  $-12$  ppm could be observed in the  $^{31}\text{P}$  MAS NMR spectra of SP-0.075 and SP-0.10. This implies that the as-synthesized SAPO-34 is mixed with some SAPO-18 crystal or CHA-AEI intergrowths occurs when the  $\text{SiO}_2/\text{Al}_2\text{O}_3$  molar ratios are 0.075 and 0.1 in the starting gel [19].

The SEM photograph of SAPO-18 with AEI topological structure is presented in Fig. 4a. The slice-like morphology can be observed. The SEM photograph of SAPO-34 as-synthesized with  $\text{SiO}_2/\text{Al}_2\text{O}_3 = 0.6$  is given in Fig. 4c. It is seen clearly that the uniform cubic-like crystals are obtained. In the Fig. 4b, for SP-0.075, some slices SAPO-18 crystals or CHA-AEI intergrowths are observed among the cubic SAPO-34 crystals.

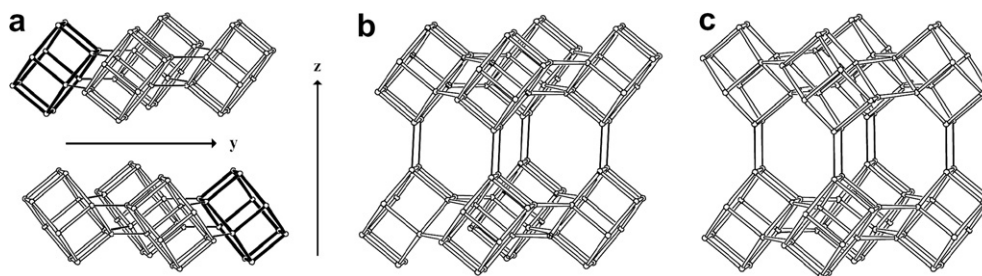


Fig. 2. Building scheme for CHA and AEI (a) periodic building unit (b) connection mode for CHA (c) connection mode for AEI.

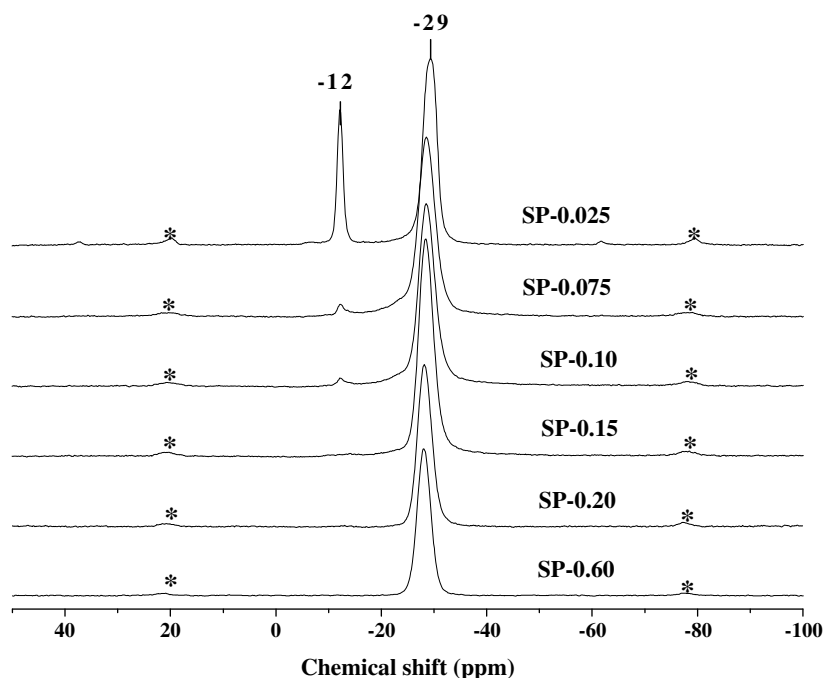


Fig. 3.  $^{31}\text{P}$  MAS NMR spectra of the as-synthesized products from the starting gel with different  $\text{SiO}_2/\text{Al}_2\text{O}_3$  ratios. (\*) indicates spinning sidebands.

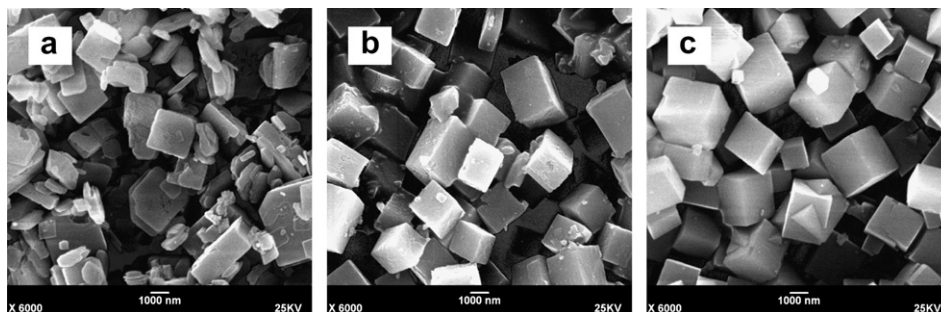


Fig. 4. SEM images of the as-synthesized products (a) SP-0.025 (b) SP-0.075 (c) SP-0.60.

### 3.2. Element composition analysis

It is known that the  $(\text{Si} + \text{P})/\text{Al}$  ratio is equal to 1 when Si is incorporated into the AlPO structure by the Si directly participating in the crystallization or by the SM2 substitution mechanism with the formation of  $\text{Si}(4\text{Al})$  species. The  $(\text{Si} + \text{P})/\text{Al}$  ratio is more than 1 when the Si is incorporated into the AlPOs structure by the SM3 substitution mechanism with the formation of  $\text{Si}(n\text{Al})$  ( $n = 3-0$ ) coordination structures. Table 1 presents molar composition of the starting gel and the as-synthesized products. In the starting gel, the molar fraction of phosphorus is equal to that of aluminum, and the  $\text{SiO}_2/\text{Al}_2\text{O}_3$  molar ratios are 0.025, 0.075, 0.10, 0.15, 0.20 and 0.60. It was seen that the Si contents of the products increased with the increase of the  $\text{SiO}_2/\text{Al}_2\text{O}_3$  molar ratios in the starting gel. The framework  $(\text{Si} + \text{P})/\text{Al}$  ratio of the products is equal to 1 when the  $\text{SiO}_2/\text{Al}_2\text{O}_3$  molar ratios of the starting gel is in the ranges of 0.075 to 0.20, which indicates that Si atoms are incorporated into the SAPO-34 framework by the Si direct participation mechanism and the SM2 substitution mode during the crystallization of SAPO-34. When  $\text{SiO}_2/\text{Al}_2\text{O}_3$  molar ratios of the starting gel was up to 0.60, the framework  $(\text{Si} + \text{P})/\text{Al}$  ratio is more than 1, implying that Si incorporation with SM3 substitution mechanisms takes place during the crystallization.

### 3.3. Si coordination structure

$^{29}\text{Si}$  MAS NMR experiments have been successfully used to determine the silicon distribution in SAPO structures [20]. Fig. 5 presents  $^{29}\text{Si}$  MAS NMR spectra of the

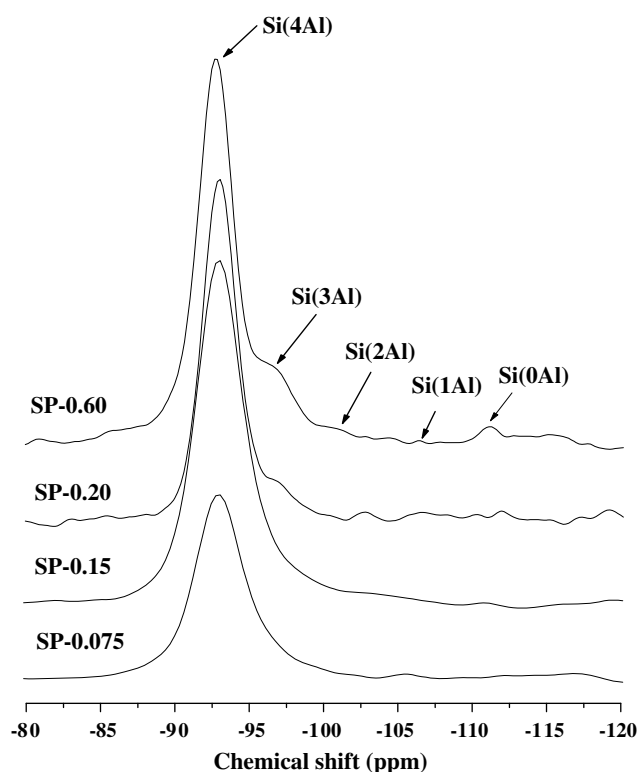


Fig. 5.  $^{29}\text{Si}$  MAS NMR spectra of the as-synthesized products from starting gel with different Si/Al ratios.

as-synthesized SAPO-34 with different  $\text{SiO}_2/\text{Al}_2\text{O}_3$  molar ratios in the starting gel. In the  $^{29}\text{Si}$  MAS NMR spectra, only one resonance peak at  $-93$  ppm is observed when the  $\text{SiO}_2/\text{Al}_2\text{O}_3$  molar ratios is less than 0.15, which comes

Table 1  
Molar composition of the initial gel and as-synthesized products

Sample	Starting gel composition		Product composition		
	Molar composition	$\text{Si}/(\text{Si} + \text{P} + \text{Al})$	Molar composition	$(\text{Si} + \text{P})/\text{Al}$	$\text{Si}/(\text{Si} + \text{P} + \text{Al})$
SP-0.025	$1.0\text{P}_2\text{O}_5:1.0\text{Al}_2\text{O}_3:0.025\text{SiO}_2$	0.006	$\text{Al}_{0.506}\text{P}_{0.487}\text{Si}_{0.007}\text{O}_2$	0.976	0.007
SP-0.075	$1.0\text{P}_2\text{O}_5:1.0\text{Al}_2\text{O}_3:0.075\text{SiO}_2$	0.018	$\text{Al}_{0.500}\text{P}_{0.470}\text{Si}_{0.030}\text{O}_2$	1.000	0.030
SP-0.10	$1.0\text{P}_2\text{O}_5:1.0\text{Al}_2\text{O}_3:0.10\text{SiO}_2$	0.024	$\text{Al}_{0.500}\text{P}_{0.464}\text{Si}_{0.036}\text{O}_2$	1.000	0.036
SP-0.15	$1.0\text{P}_2\text{O}_5:1.0\text{Al}_2\text{O}_3:0.15\text{SiO}_2$	0.036	$\text{Al}_{0.500}\text{P}_{0.447}\text{Si}_{0.053}\text{O}_2$	1.000	0.053
SP-0.20	$1.0\text{P}_2\text{O}_5:1.0\text{Al}_2\text{O}_3:0.20\text{SiO}_2$	0.048	$\text{Al}_{0.500}\text{P}_{0.440}\text{Si}_{0.060}\text{O}_2$	1.000	0.060
SP-0.60	$1.0\text{P}_2\text{O}_5:1.0\text{Al}_2\text{O}_3:0.60\text{SiO}_2$	0.130	$\text{Al}_{0.493}\text{P}_{0.413}\text{Si}_{0.094}\text{O}_2$	1.028	0.094

from the contribution of the Si(4Al) coordination. This also confirms that the Si directly participating in the crystallization or the SM2 substitution mechanism is predominant for forming Si(4Al) structure by Si–O–Al linkage. When the SiO<sub>2</sub>/Al<sub>2</sub>O<sub>3</sub> molar ratios increase to 0.20, a weak shoulder peak appears at –97 ppm in SP-0.2 sample, which corresponds to Si(3Al) coordination environment. This shows that Si incorporation by SM3 substitution mechanism takes place when the SiO<sub>2</sub>/Al<sub>2</sub>O<sub>3</sub> molar ratio is 0.20. With the increase of the SiO<sub>2</sub>/Al<sub>2</sub>O<sub>3</sub> molar ratio to 0.60, the <sup>29</sup>Si MAS NMR spectrum of as-synthesized SP-0.6 shows more resonance peaks at –101, –106, and –111 ppm, which are attributed to Si(2Al), Si(1Al) and Si(0Al) species, respectively [7,9,21]. Furthermore the shoulder peak at –97 ppm from the Si(3Al) species is intensified. This shows that Si incorporation by SM3 substitution mechanism increased during the crystallization of SP-0.6.

#### 3.4. Si incorporation mechanism

Fig. 6 lists the interrelation curve of Si content [Si/(Si + P + Al)] in the products and the starting gel. The curve can be divided into three segments, such as AB, BC and CD, respectively. Point A is the beginning of the curve, B is the intersection point of two tangents with different slope, and C is the intersection point between the curve and line  $y = x$ , in which Si content in the as-synthesized product would be equal to that in the starting gel. When the SiO<sub>2</sub>/Al<sub>2</sub>O<sub>3</sub> molar ratio is 0.025 in the starting gel, SAPO-18 molecular sieve with AEI topological structure is synthesized, and Si content in the framework is slightly higher than that in the starting gel. When the SiO<sub>2</sub>/Al<sub>2</sub>O<sub>3</sub> molar ratios were in the range of 0.075 to 0.2, CHA-AEI structure intergrowths or SAPO-34 with CHA structure are formed, and Si content in the framework is largely more than that in the starting gel (AB and BC segments).

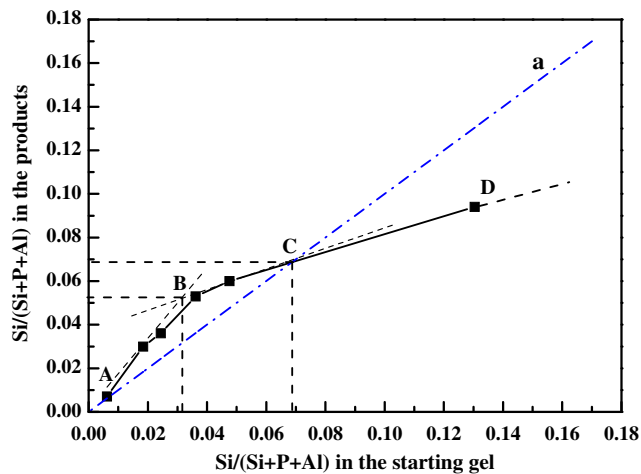


Fig. 6. Changes of Si/(Si + P + Al) in the products with Si/(Si + P + Al) in the starting gel.

When the SiO<sub>2</sub>/Al<sub>2</sub>O<sub>3</sub> ratio is up to 0.6, Si content in the framework of SAPO-34 is largely less than that in the starting gel. Meanwhile, it may be deduced that Si content of the as-synthesized SAPO-34 should be equal to that in the starting gel at point C.

In Fig. 6, it was seen that the slope of AB segment is higher than that of BC segment. This illustrates that the increase of Si content is more predominant in the AB segment, and the increase trend is weakened in the BC segment. This also shows that the ability of Si incorporation into the framework is different between AB and BC. <sup>29</sup>Si MAS NMR results indicated that only Si(4Al) was found in the structure of SP-0.075 and SP-0.10. Thus, when Si content in the starting gel is lower than the corresponding  $x$ -coordinate value of point B, all the Si atoms would take part in the SAPO-34 crystal nucleuses by the mechanism of Si directly incorporated into the framework. The framework Si content of the as-synthesized sample is largely higher than that in the starting gel. But the content of Si atoms incorporated by direct participation of the crystallization mechanism has a threshold, which is the corresponding  $y$ -coordinate value at point B. When Si content in the starting gel is higher than the corresponding  $x$ -coordinate value of point B, the increased rate of framework Si content is reduced. In the <sup>29</sup>Si MAS NMR spectra, the Si(3Al) structure is found in SP-0.20 sample, and SM3 and SM2 substitution mechanisms took place for samples with a Si/Al-ratio in the range of the line BC. In other words, when the Si content in the starting gel is more than the corresponding  $x$ -coordinate value of B point, part of Si atoms took part in the SAPO-34 crystal nucleation by the mechanism of Si directly incorporated into framework, when the framework Si content is up to the corresponding  $y$ -coordinate value of B point, the residual Si atoms in the gel are incorporated into SAPO-34 framework by SM2 and SM3 substitution mechanism. When Si content in the starting gel continues to increase (CD segment), the framework Si content in the as-synthesized product is smaller than that in the starting gel. This could be explained by an increase in the proportion of SM3 substitution mechanism, and Si(3Al), Si(2Al), Si(1Al) and Si(0Al) coordination environments were formed.

In summary, the modeling of Si incorporation into SAPO-34 framework varies with Si content in the starting gel. When Si content in the starting gel is less than the abscissa value of point B [Si/(Al + P + Si) = 0.031], Si, P and Al directly form the SAPO-34 framework with Si(4Al) coordination environment. When Si content in the gel is higher than the abscissa value of point B, some Si atoms are incorporated into the SAPO-34 framework by direct participation of the crystallization with the formation of isolated and well-distributed Si(4Al) species, with the amount of Si atoms in the framework increasing to the threshold [Si/(Al + P + Si) = 0.052], the remaining Si atoms entered the framework by combined SM2 and SM3 substitution mechanisms to form Si( $n$ Al) species.

#### 4. Conclusions

Si contents in the starting gel had crucial effect on Si atoms incorporation modeling and Si coordination environment during SAPO-34 crystallization. When Si content in the starting gel was smaller than a threshold [ $\text{Si}/(\text{Al} + \text{P} + \text{Si}) = 0.031$ ], all Si atoms took part in the SAPO-34 crystal nucleuses by the mechanism of the direct participation crystallization and only Si(4Al) was found in the framework; When Si content in the starting gel was more than the threshold, part of Si atoms took part in the SAPO-34 crystal nucleuses by the mechanism of Si directly incorporated into the framework, the residual Si atoms in the gel were incorporated into SAPO-34 framework by combined SM2 and SM3 substitution mechanisms and Si(3Al), Si(2Al), Si(1Al) and Si(0Al) coordination environments were formed.

#### References

- [1] J. Liang, H.-Y. Li, S.-Q. Zhao, W.-G. Guo, R.-H. Wang, M.-L. Ying, *Appl. Catal.* 64 (1990) 31.
- [2] Y. Xu, C.P. Grey, J.M. Thomas, A.K. Cheetham, *Catal. Lett.* 4 (1990) 251.
- [3] T. Inui, in: H. Chon, S.-K. Ihm, Y.S. Uh (Eds.), *Proceedings of the 11th International Zeolite Conference, Progress in Zeolite and Microporous Materials, Studies in Surface Science and Catalysis, Part B*, vol. 105, Elsevier, Amsterdam, 1997, p. 1441.
- [4] G. Sastre, D.W. Lewis, C.R.A. Catlow, *J. Phys. Chem. B* 101 (27) (1997) 5249.
- [5] R. Vomscheid, M. Briend, M.J. Peltre, P.P. Man, D. Barthomeuf, *J. Phys. Chem.* 98 (1994) 9614.
- [6] E. Dumitriu, A. Azzouz, V. Hulea, D. Lutic, H. Kessler, *Micropor. Mater.* 10 (1–3) (1997) 1.
- [7] S. Ashtekar, S.V.V. Chilukuri, D.K. Chakrabarty, *J. Phys. Chem.* 98 (1994) 4878.
- [8] B. Chakraborty, A.C. Pulikottil, B. Viswanathan, *Appl. Catal. A* 167 (1998) 173.
- [9] A.M. Prakash, S.J. Unnikrishnan, *Chem. Soc. Faraday Trans.* 90 (1994) 2291.
- [10] D. Barthomeuf, *Zeolites* 14 (1994) 394.
- [11] J. Tan, Z.-M. Liu, X.-H. Bao, X.-C. Liu, X.-W. Han, C.-Q. He, R.-S. Zhai, *Micropor. Mesopor. Mater.* 53 (2002) 97.
- [12] M. Hunger, M. Seiler, A. Buchholz, *Catal. Lett.* 74 (2001) 61.
- [13] C. Kladis, S.K. Bhargava, D.B. Akolekar, *J. Mol. Catal. A: Chem.* 203 (2003) 193.
- [14] R. Wendelbo, D. Akporiaye, A. Andersen, I.M. Dahl, H.B. Mostad, *Appl. Catal. A: Gen.* 142 (1996) L197.
- [15] H.-Y. He, J. Klinowski, *J. Phys. Chem.* 97 (1993) 10385.
- [16] J.-S. Chen, P.A. Wright, J.M. Thomas, S. Natarajan, L. Marchese, S.M. Bradley, G. Sankar, C.R.A. Catlow, P.L. Gai-Boyes, R.P. Townsend, C.M. Lok, *J. Phys. Chem.* 98 (1994) 10216.
- [17] H. van Koningsveld, Schemes for building zeolite framework models. <<http://www.iza-structure.org/databases/>>.
- [18] A. Simmen, L.B. McCusker, C. Barlocher, W.M. Meier, *Zeolites* 11 (1991) 654.
- [19] M.J.G. Janssen, A. Verberckmoes, M.M. Mertens, A.J. Bons, W.J. Mortier, US Patent 6,953,767, 2002.
- [20] D. Freude, H. Ernst, M. Hunger, H. Pfeifer, E. Jahn, *Chem. Phys. Lett.* 143 (1988) 477.
- [21] R.B. Borader, A. Clearfield, *J. Mol. Catal.* 88 (1994) 249.